

**FREQUENCY CONVERSION OF COHERENT IMAGES ON INTRACAVITY MULTIWAVE MIXING
CONVERSIÓN DE FRECUENCIA DE IMÁGENES COHERENTES DENTRO DE UNA CAVIDAD CON
MEZCLA DE MUCHAS ONDAS**

Omar Ormachea, Oleg G. Romanov* and Alexei L. Tolstik*

Centro de Investigaciones Ópticas - CIO

Universidad Privada Boliviana

** Universidad Estatal de Bielorrusia*

oormachea@upb.edu

(Recibido el 7 de noviembre 2009, aceptado para publicación el 21 de diciembre 2009)

ABSTRACT

The schemes for recording and reading of dynamic holograms in conditions of nondegenerate four- and six-wave mixing in a nonlinear Fabry-Perot interferometer have been analyzed theoretically. It has been demonstrated that there is a possibility for a considerable improvement in the diffraction efficiency and angular selectivity of dynamic gratings in the interferometer compared to the off-cavity interaction. A method for the frequency conversion of coherent images with simultaneous phase conjugation has been realized experimentally.

RESUMEN

Los esquemas de registro y reconstrucción de hologramas dinámicos, en condiciones de mezcla de cuatro y de seis ondas no degenerado, dentro de un interferómetro del tipo Fabry-Perot no lineal, se han analizado teóricamente. Se ha demostrado que existe la posibilidad de que una considerable mejora en la eficiencia de difracción y de la selectividad angular de las rejillas dinámicas dentro de un interferómetro en comparación con la interacción fuera de este tipo de cavidad. Un método para la conversión de frecuencia de imágenes coherentes, con conjugación de fase simultánea, se ha realizado experimentalmente.

Keywords: Dynamic Holography, Frequency Conversion of Images, Nondegenerate Multiwave Mixing, Nonlinear Interferometer.

Palabras Clave: Holografía Dinámica, Conversión de Frecuencia de Imágenes, Mezcla de Muchas Ondas Nodegenerado, Interferómetro Nolineal.

1. INTRODUCCION

Extension of a theory for the formation and interaction of light beams in distributed nonlinear systems (e. g., nonlinear Fabry-Perot interferometer) is of great importance for the basic and applied research. The results of the related studies may be used for the development of new optical switchable devices, high-speed data processing systems, optical memories, etc. [1].

The use of an optical cavity in the schemes for recording of stationary [2] and dynamic [3], [4] holograms in semiconductor materials [5], solutions of complex organic compounds [6], [7], amplifying media [8] has demonstrated the possibility for a considerable improvement in the light-field transformation efficiency in conditions of Bragg diffraction. The advantages of optical cavities are particularly important for realization of the frequency-degenerate intracavity light-wave mixing [9] in the case when the intracavity feedback is effected for a reading light beam.

This paper presents a theoretical and experimental study into the efficiency of the coherent-image frequency conversion processes on multiwave interactions in Fabry-Perot interferometer, with the solutions of complex organic compounds (dyes) used as a nonlinear medium.

**2. THEORETICAL MODEL FOR FREQUENCY-NONDEGENERATE MULTIWAVE INTERACTIONS IN
NONLINEAR INTERFEROMETER**

A theoretical model describing the nondegenerate multiwave mixing is based on a system of coupled wave equations for the complex amplitudes of light waves in the conditions when dynamic gratings are recorded by the signal E_S and reference E_1 waves at the frequency ω , whereas reading is performed by the wave E_2 at the doubled frequency 2ω .

Depending on the propagation direction of a reading wave, one can realize four- (Figure1a) or six-wave (Figure1b) mixing.

In the first case, the nonlinear polarization responsible for the formation of the diffracted wave E_D at the frequency 2ω is of the form $P \propto E_1 E_s^* E_2$, the phase synchronism condition $\vec{k}_1 + \vec{k}_2 = \vec{k}_s + \vec{k}_D$ being associated with a decrease of an angle between the diffracted and reading beams relative to that formed by the hologram recording waves. Nonlinear polarization for the scheme of six-wave mixing is represented as $P \propto (E_1 E_s^*)^2 E_2$, and the diffracted wave E_D propagation direction is determined by the phase synchronism condition $\vec{k}_D = 2\vec{k}_1 - 2\vec{k}_s + \vec{k}_2$. Note that in terms of dynamic holography, the matter concerns recording and reading of linear (four-wave mixing) and quadratic (six-wave mixing) dynamic holograms [10]. With opposite propagation directions of the plane reference E_1 and reading E_2 waves ($2\vec{k}_1 + \vec{k}_2 = 0$), the diffracted wave E_D has characteristics of a phase conjugate to the signal wave E_s , because it is propagating exactly in the counter direction ($\vec{k}_D = -2\vec{k}_s$) at the conjugate wave front ($\varphi_D = -2\varphi_s$). So in this interaction geometry one can realize frequency conversion of complex wave fronts enabling visualization, e.g., of infrared (IR) images [11].

To describe theoretically the energy efficiency of interaction, let us assume that recording of dynamic gratings is realized at the frequency coincident with the absorption line center $S_0 - S_1$ of a dye solution. The medium is absorbing radiation at the frequency ω , being transparent at the doubled frequency 2ω . Forming of the wave E_D is determined by diffraction of the reading wave E_2 from a thermal dynamic grating recorded by the signal and reference waves.

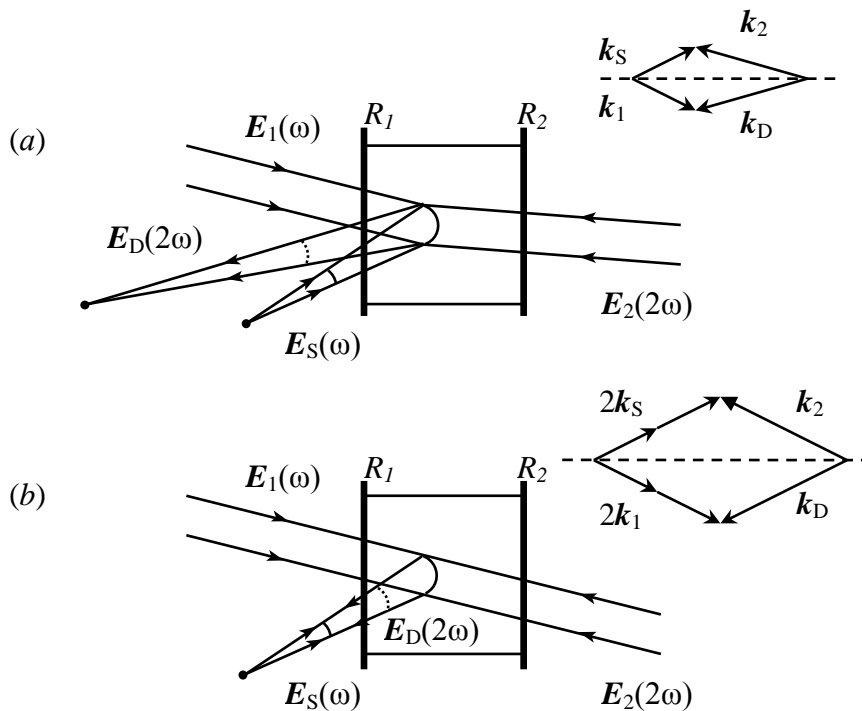


Figure 1 - Schemes for transformation of light beams on the frequency-nondegenerate four- (a) six-wave (b) mixing.

Taking into consideration the absorption saturation effect in the principal spectral channel $S_0 - S_1$ and induced absorption from the excited channel S_1 characteristic for solutions of complex organic compounds (dyes), one can derive expressions for nonlinear susceptibility of the medium at the fundamental and doubled frequency as follows [12]:

$$\chi(\omega) = \frac{n_0 K_0}{2\pi} \left(\frac{\hat{\Theta}_{12}}{B_{12}} - \frac{\hat{\alpha}I - b_r I^2}{1 + JI} \right), \quad (1)$$

$$\chi(2\omega) = \frac{n_0 \kappa_0}{2\pi} \left(\frac{a_T I + b_T I^2}{1 + JI} \right). \quad (2)$$

Here $\hat{\alpha} = a + i\alpha = (\hat{\Theta}_{12} + \hat{\Theta}_{21} - \hat{\Theta}_{23})/\nu P_{21} - a_T$, $b_T = \sigma_T B_{23} (1 - \mu_{32})/\nu P_{21}$, $a_T = \sigma_T (1 - \mu_{21})$, $J = (B_{12} + B_{21})/\nu P_{21}$.

In these expressions $\hat{\Theta}_{kl}(\omega) = \Theta_{kl}(\omega) + iB_{kl}(\omega)$, where the coefficients $\Theta_{kl}(\omega)$ are related by Kramers-Kronig relations to Einstein's coefficients for the induced transitions $B_{kl}(\omega)$, κ_0 – initial extinction coefficient, n_0 – initial refractive index; $\nu = c/n_0$ – speed of light in the medium, P_{21} – total probability of spontaneous and nonradiative transitions between the levels $S_0 - S_1$; $\sigma_T = 2\omega(dn/dT)\tau/cC_\rho$, τ – interaction duration, C_ρ – unit volume thermal capacity, dn/dT – thermo optical coefficient, μ_{kl} – luminescence quantum efficiency in the channel $k - l$.

In the approximation of slowly varying light-field amplitudes, the equations for complex amplitudes may be written in the following way:

$$\begin{cases} \frac{\partial E_{1,S}}{\partial z} = \frac{i2\pi\omega}{cn_0} \{ \chi_0(\omega) E_{1,S} + \chi_{\pm 1}(\omega) E_{S,1} \} \\ \frac{\partial E_{2,D}}{\partial z} = -\frac{i4\pi\omega}{cn_0} \{ \chi_0(2\omega) E_{2,D} + \chi_{\mp m}(2\omega) E_{D,2} \} \end{cases}, \quad (3)$$

where the components of the nonlinear-susceptibility series expansion in terms of spatial harmonics of a holographic grating are calculated using the Fourier transform $\chi_m = \frac{1}{2\pi} \int_{-\pi}^{\pi} \chi(\zeta) \exp[-i(m\zeta)] d\zeta$, $\zeta = (\vec{k}_1 - \vec{k}_s) \cdot \vec{r}$. With this system of equations one can describe the process of frequency-degenerate four-wave mixing for $m=1$ and also the process of nondegenerate six-wave mixing at $m=2$.

Considering the explicit form of expressions for the medium's nonlinear susceptibility Fourier-components $\chi_{\pm 1, \pm 2}$, a system of coupled wave equations (3) may be transformed to

$$\begin{cases} \frac{\partial E_{1,S}}{\partial z} = i \frac{k_0}{2} f_{1,S} E_{1,S} \\ \frac{\partial E_{2,D}}{\partial z} = -ik_0 (\psi^{(m)} E_{2,D} + \phi^{(m)} E_{D,2} \exp[\mp im(\varphi_1 - \varphi_s)]) \end{cases}, \quad (4)$$

where the following notation is used:

$$\begin{cases} f_{1,S} = \frac{\hat{\Theta}_{12}}{B_{12}} + \frac{b_T(I_{1,S} + 2I_{1,S})}{J} - \frac{\hat{\alpha} + b_T/J}{J} \left(1 - \frac{1}{A_0} + \frac{2JI_{1,S}}{A_0(1 + J(I_1 + I_S) + A_0)} \right) \\ \psi^{(1)} = b_T(I_1 + I_S)/J + (a_T - b_T/J)(1 - 1/A_0)/J \\ \psi^{(2)} = (a_T - b_T/J)(1 - 1/A_0)/J \\ \phi^{(1)} = \frac{b_T}{J} \sqrt{I_1 I_S} + \frac{2(a_T - b_T/J) \sqrt{I_1 I_S}}{A_0(1 + J(I_1 + I_S) + A_0)} \\ \phi^{(2)} = -\frac{4(a_T - b_T/J) I_1 I_S}{A_0(1 + J(I_1 + I_S) + A_0)^2} \\ A_0 = \left(1 + 2J(I_1 + I_S) + J^2(I_1 - I_S)^2 \right)^{1/2} \end{cases}$$

The coefficients f_1 and f_S include the absorption factor and refractive index modulation in the interference field as well as self-diffraction of the reference and signal waves; self-modulation is described by the expressions $\psi^{(1),(2)}$ and $\phi^{(1),(2)}$ is used to describe the parametric coupling of the reading and diffracted waves in the case of four - ($m=1$) and six-wave ($m=2$) mixing.

To realize effective reading of the dynamic gratings recorded by the waves E_S and E_1 at the frequency ω , it is proposed [9] to use the cavity feedback for the reading E_2 and diffracted E_D waves at the doubled optical frequency 2ω .

With due regard for multiple reflections from mirrors of the Fabry-Perot interferometer, an amplitude of the reading wave E_2 at the output may be found as a sum of the waves representing a geometrical progression

$$E_{2T} = E_{20} \sqrt{1-R_2} \exp(i\Phi_2) \sqrt{V} \sqrt{1-R_1} \times \left\{ 1 + V \sqrt{R_1 R_2} \exp(i2\Phi_2) + V^2 R_1 R_2 \exp(i4\Phi_2) + \dots \right\}, \quad (5)$$

where E_{20} – amplitude of the reading wave at the cavity input, R_1 and R_2 – reflection factors of the cavity mirrors, $\Phi_2 = \frac{2\pi}{\lambda} nL \cos \theta_2$ – phase shift of the wave E_2 propagating at the angle θ_2 to the cavity axis z , L – cavity length, V – coefficient determining intensity losses for the wave E_2 in one pass of the cavity. And an intensity of the wave E_2 at the cavity output may be determined as

$$I_{2T} = cn_0 |E_{2T}|^2 / 8\pi = I_{20} \frac{(1-R_1)(1-R_2)V}{(1-\sqrt{R_1 R_2} V)^2 + 4\sqrt{R_1 R_2} V \sin^2(\Phi_2)}, \quad (6)$$

where $I_{20} = cn_0 |E_{20}|^2 / 8\pi$ – intensity of the input reading wave. In case there is no absorption at the frequency 2ω , losses of the reading wave are governed by its diffraction from the dynamic grating recorded within the interferometer $V = 1 - \xi_0$, $\xi_0 = I_D(z=0)/I_{20}$ being the diffraction efficiency of dynamic gratings in one pass of a nonlinear layer.

In a similar way, summing up the wave amplitudes due to diffraction of the wave E_2 from the intracavity grating in every pass of the cavity, one can find the diffracted wave amplitude at the interferometer output as

$$E_{DT} = E_D(z=0) \sqrt{1-R_1} \times \left\{ 1 + VV^* \sqrt{R_1 R_2} \exp(i2\Phi_D) + V^2 (V^*)^2 R_1 R_2 \exp(i4\Phi_D) + \dots \right\}, \quad (7)$$

where $E_D(z=0)$ is the amplitude of the diffracted wave in a one pass of a nonlinear layer determined by solving a system of equations (4), $\Phi_D = \frac{2\pi}{\lambda} nL \cos \theta_D$ is the phase shift of the diffracted wave propagating at the angle θ_D relative to the cavity axis z . The one-pass diffracted wave amplification is determined by the parameter $V^* = 1 + \xi_0$.

Based on expression (7), the diffraction efficiency of the reading wave E_2 at the intracavity grating may be as

$$\xi_R = \frac{|E_{DT}|^2}{|E_{20}|^2} = \xi_0 \frac{(1-R_1)}{(1-\sqrt{R_1 R_2} VV^*)^2 + 4\sqrt{R_1 R_2} VV^* \sin^2(\Phi_D)}. \quad (8)$$

As follows from analysis of expression (8), a maximum gain in the diffraction efficiency at a symmetric configuration of the cavity ($R_1 = R_2 = R$) may be attained when the interferometer is tuned to a maximum transmission ($\Phi_D = 0$) and, in the region of small ξ_0 , may be evaluated from a simple relation $\xi_R \approx \xi_0 / (1-R)$. Thus, due to the cavity coupling for the wave E_2 , a dynamic grating may be reread many times with the increased energy contribution from the wave E_2 that is transformed to the diffracted wave E_D .

Numerical modeling for the equations of (4) with regard to expressions (6) - (8) has been performed, using the following spectral and thermo optical characteristics of the medium associated with 3274U dye in ethanol solution, in the assumption of laser excitation into the absorption line center $S_0 - S_1$ [14]: ($\lambda = 1064$ nm, pulse length $\tau = 15$ ns, $n_0 = 1.36$, $dn/dT(C_p)^{-1} = -2 \cdot 10^{-4} J^{-1} cm^3$, $B_{23}/B_{12} = 0.43$, with Stokes shift assumed to be equal to the absorption line halfwidth $\Delta\lambda = 100$ nm, luminescence quantum efficiency $\mu_{12} = 0.01$, $\mu_{32} = 0.0001$).

The calculation results for the diffraction efficiency of dynamic gratings at the frequency 2ω are shown in Figure 2 depending on the intensity of the hologram recording waves at different reflection factors of the cavity mirrors. The functions have been obtained when the Fabry-Perot interferometer was tuned to a maximum transmission of the waves E_2 and E_D ($\Phi_{2,D} = 0$). Note a significant improvement in the diffraction efficiency of intracavity dynamic gratings as

compared to the classical scheme without a cavity, particularly in the region of low intensities, where the use of high-reflection mirrors $R \approx 0.9$ leads to a diffraction efficiency increase approximating the above estimate $\xi_R \approx \xi_0/(1-R)$.

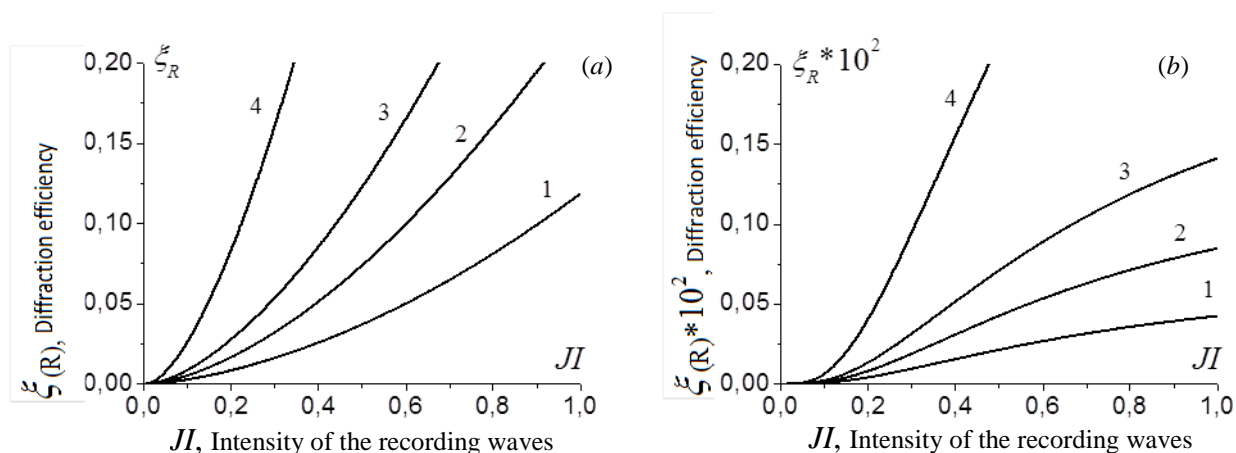


Figure 2 - Diffraction efficiency ξ versus intensity of the waves recording dynamic gratings, for linear (a) and quadratic recording (b); $k_0L=1$, $R_1=R_2=0$ (1), 0.5 (2), 0.7 (3), 0.9 (4).

Another feature of using the intracavity schemes for dynamic hologram recording is an enhancement of their angular and spectral selectivity [6] because of the increasing effective length of the interacting light beams. Let us compare the dynamic hologram selecting properties for the above-mentioned schemes of intracavity and off-cavity four- and six-wave mixing. A system of wave equations (4) in the case of minor deviation from the phase synchronism conditions may be rewritten as

$$\begin{cases} \frac{\partial E_{1,s}}{\partial z} = i \frac{k_0}{2} f_{1,s} E_{1,s} \\ \frac{\partial E_{2,D}}{\partial z} = -ik_0 (\psi^{(m)} E_{2,D} + \phi^{(m)} E_{D,2} \exp[\mp im(\varphi_1 - \varphi_s \pm \Delta kz)]) \end{cases}, \quad (9)$$

where the deviation of a reading wave from the exactly fulfilled Bragg diffraction condition is determined by the parameter $\Delta k = 2 \frac{\omega}{c} \theta \Delta \theta$.

Figure 3 presents the diffraction efficiency of dynamic gratings as a function of the angle of the reading-wave deviation from the Bragg resonance conditions $\Delta \theta$ obtained from numerical solution of a system of wave equations (9) for the cases of four- and six-wave mixing in off-cavity (a) and intracavity (b) geometries. All the functions are normalized to their maximum values. The calculations are performed using the interferometer parameters ($L = 500 \mu\text{m}$ at $R_1 = R_2 = 68\%$) involved subsequently in the experimental studies.

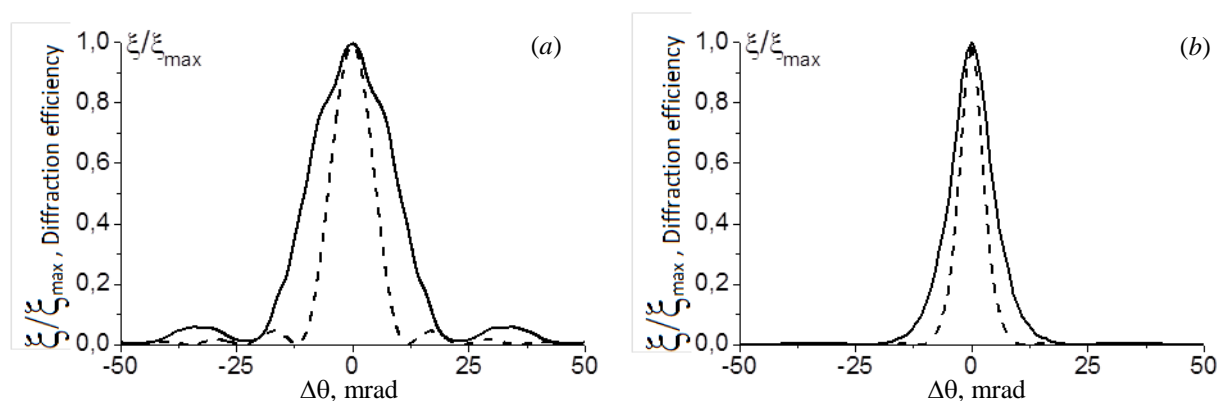


Figure 3 - Diffraction efficiency ξ versus deviation of the reading wave from the Bragg resonance condition $\Delta \theta$: (a) - off- and (b) - intracavity geometries for four - (solid lines) and six-wave (broken lines) mixing; $k_0=20 \text{ cm}^{-1}$, $\theta=45 \text{ mrad}$, $L=500 \mu\text{m}$, $R_1=R_2=68\%$.

The following features of the functions obtained are noticeable. First, an angular width of the resonance peak for the case of six-wave mixing ($\Delta\theta_{0,5} \approx 10$ mrad) is only a half of that in the process of four-wave mixing ($\Delta\theta_{0,5} \approx 20$ mrad) (Figure 3a) due to the doubly decreased period of the volume dynamic hologram participating in the process of Bragg diffraction upon the associated change in the diffraction order. With the parameters used ($\Lambda \approx 10 \mu\text{m}$, $L = 500 \mu\text{m}$), the derived values are in a good agreement with the well-known expression for the angular selectivity of holographic gratings: $\Delta\theta_{0,5} \approx \frac{\Lambda}{L}$ ($\Lambda = \frac{\lambda}{2 \sin \theta}$ - grating period) that is valid for small deviations in propagation of the reading wave from Bragg condition and for lacking of absorption at a frequency of the reading wave [14]. Second, the use of the interferometer with the reflection factors of mirrors $R_1 = R_2 = 68\%$ results in a practically two-fold narrowing of the angular selectivity peak for dynamic gratings (Fig.3b) caused by the increased effective interaction length of light beams following from expression (6): $L_{\text{eff}} \approx L_0 \frac{\sqrt{1-R_1}}{1-\sqrt{R_1 R_2}}$. On the one hand, this situation may lead to the degraded transformation quality of complex wave fronts but, on the other hand, it may be employed to realize multiplex recording of dynamic holograms.

3. EXPERIMENTAL STUDY OF THE PROCESS OF IMAGE FREQUENCY CONVERSION

An experimental setup used to study the frequency-nondegenerate interaction in a nonlinear Fabry-Perot interferometer is demonstrated in Figure 4a.

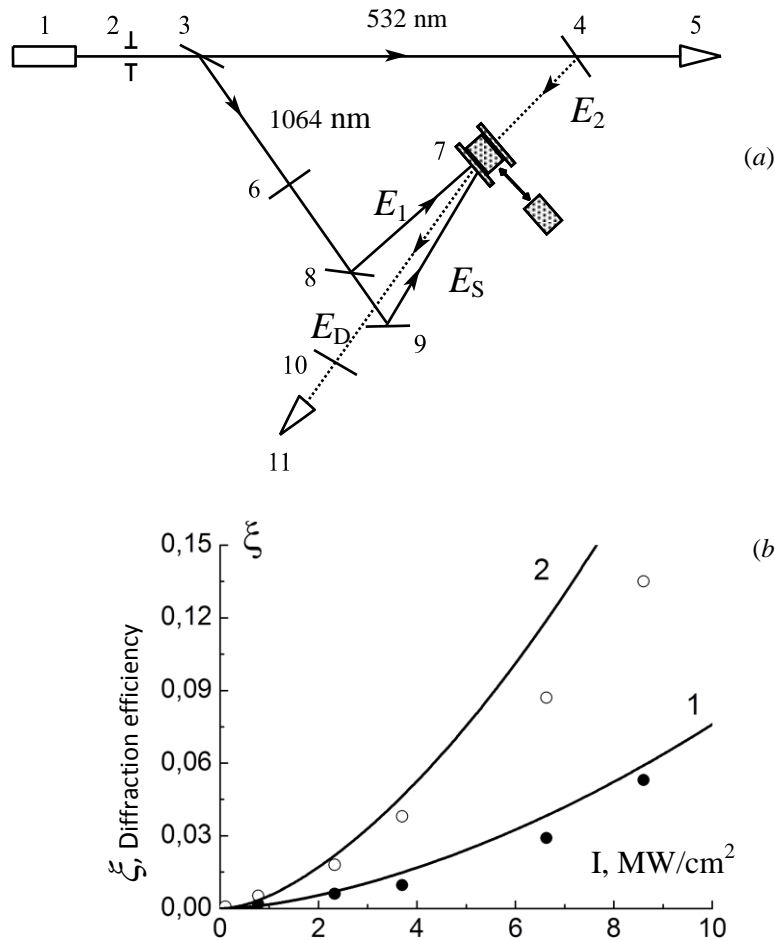


Figure 4 - (a) experimental setup; (b) diffraction efficiency versus intensity of the waves recording dynamic gratings; (1) off and (2) intra -cavity four-wave mixing.

The study was performed using the ethanol solution of 3274U dye, the fundamental- ($\lambda = 1064$ nm) and second ($\lambda = 532$ nm) harmonic radiation of yttrium-aluminum garnet laser 1 ($\tau = 15$ ns). The absorption band of 3274U dye is exhibited at the fundamental lasing frequency (saturation intensity $I_{Sat} \approx 13$ Mw/cm², molecular lifetime in the excited singlet state $\tau_{21} \approx 10$ ps [15]), the dye being practically transparent at the second-harmonic frequency and enabling one to record dynamic holograms in the IR spectral region with their reconstruction in the visible. The selected diffraction scheme of laser radiation in the Bragg mode is realized with the co-propagating signal and reference waves. Diaphragm 2 cuts the spatially homogeneous portion of radiation from the yttrium-aluminum garnet laser. The signal E_s and reference E_1 waves are formed by mirrors 3, 8, and 9. Owing to the angle $2\theta \approx 90$ mrad formed between propagation directions of the reference and signal beams, the interacting waves may be overlapping over the whole cell length. With the help of mirror 4, the reading wave E_2 is directed into the nonlinear medium 7. The energy efficiency of the interacting light beams is measured by recording system 5, 11. Light filters 6, 10 are used to change the power of laser radiation.

The main task of this experimental study is comparison between the diffraction efficiencies of dynamic gratings when nondegenerate multiwave mixing is realized in the off-cavity scheme as well as with the use of a Fabry-Perot interferometer. To this end, we use a cell with the thickness $L=500\mu\text{m}$ and Fabry-Perot interferometer with the same cavity base and mirror reflection factors $R_1 = R_2 = 68\%$ at a wavelength of 532 nm. An optical thickness of the 3274U dye solution at $\lambda = 1064$ nm in both cases comes to $k_0L=1$. Note that the interferometer is intended for the radiation wavelength $\lambda = 532$ nm, whereas (signal E_s and reference E_1) waves of the fundamental lasing frequency are transmitted through the nonlinear medium without the cavity feedback. The diffraction efficiency of holographic gratings is measured using for recording the spatially homogeneous light beams of the same intensity.

Owing to the performed study, the prospects for improvement of the dynamic-grating diffraction efficiency have been demonstrated experimentally using the schemes of intracavity four- and six-wave mixing. Figure 4b shows the diffraction efficiency ($\xi = I_D(z=0)/I_2(z=L)$) as a function of the intensity of the dynamic-grating recording waves E_s and E_1 in case of four-wave mixing. As seen, an increase in the diffraction efficiency with growing intensity is practically quadratic, amounting to a few tens percent. In the process, the use of intracavity interactions (curve 2) enables one to double or treble the diffraction efficiencies compared to the off-cavity case (curve 1), making it possible to attain experimental diffraction efficiencies $\approx 13.5\%$.

Solid lines in Figure 4b represent the results of numerical modeling based on a system of equations (4), (8) with the radiation and nonlinear interferometer parameters meeting the experimental conditions. By the introduction of the effective interaction time ($\tau_{eff} = \tau/\sqrt{3}$) during the calculations one can take account of the fact that the numerical solution gives a value of the diffraction efficiency by the end of a pulse, while the experiment provides the pulse-averaged diffraction efficiency. By this assumption it is possible to have a reasonable agreement between the experimental data and theoretical results.

Fairly high experimental diffraction efficiencies make it possible to realize frequency conversion of the coherent images formed when the amplitude transparencies are brought about into the signal beam. With the use of both configurations for the light beam interactions (four- and six-wave mixing), the IR-to-visible conversion of images has been realized experimentally, Figure 5.

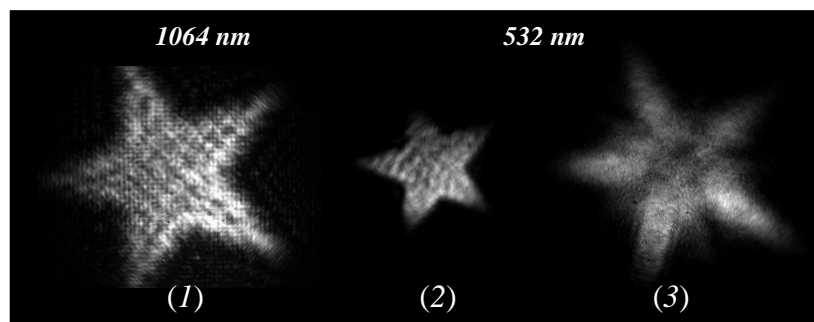


Figure 5 - Visualized IR image (1) in the case of four- (2) and six-wave (3) mixing.

A dynamic hologram of the image (1) formed at the wavelength $\lambda = 1064$ nm is recorded by the reference E_1 and signal E_s light beams. Depending on the interaction geometry, reading of the hologram by the beam E_2 at $\lambda = 532$ nm enables reconstruction of the first- (2) or second-order (3) diffraction, in the latter case with simultaneous phase conjugation at the doubled optical frequency.

4. CONCLUSIONS

The theoretical and experimental studies performed demonstrate that using of the schemes for intracavity light-beam interactions permits the diffraction efficiency of intracavity dynamic gratings to be improved considerably as a result of a constructive interference on multiple diffraction of the reading wave in a nonlinear layer of the cavity. High diffraction efficiency (up to 13.5%) with simultaneous infrared-to-visible frequency conversion of coherent images has been experimentally obtained by intracavity nondegenerate four-wave mixing.

5. REFERENCES

- [1] N.N. Rosanov. *Optical bistability and hysteresis in distributed nonlinear systems* (M.: Nauka. 1997).
- [2] A. Sinha and G. Barbastathis. *Optics Letters*. Vol. 27, pp. 385, 2002.
- [3] L. Menez et al. *Opt. Soc. Am. B*, 16, pp. 1849, 1999.
- [4] R. Buhleier et al. *Applied Physics Letters* 69, pp. 2240, 1996.
- [5] V.M. Petrov et al. *Thin Solid Films*. 450, pp. 178, 2004.
- [6] L. Menez et al. *Optics Letters*. 27, pp. 479, 2002.
- [7] O. Ormachea et al. *Proceedings of SPIE* 5949, pp. 261, 2005.
- [8] A. Moreau et al. *Optics Letters*. 32, pp. 208, 2007.
- [9] O. Ormachea et al. *Optics Express* 14, pp. 8298, 2006.
- [10] S.M. Karpuk et al. *Bulletin of the Russian Academy of Sciences. Physics. Supplement: Physics of Vibration* 60, pp. 52, 1996.
- [11] S.M. Karpuk et al. *Optics and Spectroscopy* 80, pp. 313, 1996.
- [12] A.S., Rubanov et al. *Optics Communications* 181, pp. 183, 2000.
- [13] M. Born and E. Wolf. *Principles of Optics. Electromagnetic Theory of Propagation, Interference and Diffraction of Light*, Pergamon Press, Oxford 1964.
- [14] R.J. Collier et al. *Optical Holography*, Academic Press 1971.
- [15] A.V. Masalov et. al *Quantum electronics* 18, pp. 749, 1991.